

## **Optics Letters**

## Low-complexity equalizer with a hybrid decision scheme for 50 Gb/s/ $\lambda$ PAM4-PON using a low-cost 10 G receiver

XIZI TANG,<sup>1,2</sup> YOU-WEI CHEN,<sup>2</sup> RUI ZHANG,<sup>2</sup> SHUANG YAO,<sup>2</sup> QI ZHOU,<sup>2</sup> SHUYI SHEN,<sup>2</sup> MENGQI GUO,<sup>1</sup> YAOJUN QIAO,<sup>1,\*</sup> AND GEE-KUNG CHANG<sup>2</sup>

<sup>1</sup> State Key Laboratory of Information Photonics and Optical Communications, School of Information and Communication Engineering, Beijing University of Posts and Telecommunications (BUPT), Beijing 100876, China

Received 29 June 2020; revised 29 August 2020; accepted 2 October 2020; posted 7 October 2020 (Doc. ID 401437); published 13 November 2020

In this Letter, we experimentally demonstrate a 50 Gb/s/ $\lambda$ four-level pulse amplitude modulation-based passive optical network system with a 10 G class receiver. A memory polynomial equalizer (MPE) combined with a decision feedback equalizer (DFE) is applied to eliminate channel distortions in the system. To further improve the performance of the MPE-DFE, for the first time, to the best of our knowledge, a low-complexity hybrid decision scheme (HDS) is proposed, which consists of single-symbol decision (SSD) and multi-symbol decision (MSD). The SSD is exactly the conventional hard decision based on minimum Euclidean distance, whereas MSD is based on a simplified maximum likelihood detection principle with M-algorithm. In terms of complexity, MSD requires 19.1% more multiplications than SSD, but the symbol number of MSD only accounts for less than 20% of the total signal frame when the received optical power is greater than -27 dBm. Experimental results show that the proposed MPE-DFE with HDS achieves a 0.7 dB and 1.3 dB sensitivity gain compared with conventional SSD, and up to 35.4 dB and 31.4 dB link power budget, regarding the forward error correction threshold of  $10^{-2}$  and  $10^{-3}$ , respectively. © 2020 Optical Society of America

https://doi.org/10.1364/OL.401437

Driven by the bandwidth-thirsty applications such as ultra-high definition video, virtual and augmented reality (VR/AR), and cloud computing services, optical access networks require an increasingly higher line-rate [1]. Time division multiplexed passive optical network (TDM-PON) based on a point-to-multipoint (PtMP) power splitting scheme has been widely deployed for optical access networks [2]. Currently, the Institute of Electrical and Electronics Engineers (IEEE) 802.3ca Task Force is setting standards for 25 G/50 G E-PON, while the International Telecommunication Union (ITU)-T Q2/SG15 has started to discuss the standards for a single wavelength 50 Gb/s PON, which can also potentially reach 100 Gb/s PON

by bonding two wavelength channels [3,4]. Since PON is cost sensitive, intensity modulation and direct detection (IM/DD) systems are still promising in single wavelength 50 Gb/s PON deployment with low cost, low power consumption, and small form size [5,6]. However, IM/DD systems suffer from channel distortions which mainly come from chromatic dispersion (CD) of fiber, nonlinear response of optical/electrical devices, as well as insufficient system bandwidth when leveraging low-cost and low-bandwidth devices to achieve a high-speed PON [7].

Recently, digital signal processing (DSP) techniques, such as advanced modulations and electrical equalizations, have been widely investigated for high-speed PON systems. For instance, Ref. [8] compared O-band 50 Gb/s/λ TDM-PON with two well-known modulation formats including four-level pulse amplitude modulation (PAM4) and discrete multi-tone (DMT). Besides, an optical amplifier has been introduced at the receiver side to extend the power budget. Ref. [9] demonstrated a symmetrical 50 Gb/s/λ PAM4-PON supporting a PR-30 link loss budget with semiconductor optical amplifier and DSP. These works are implemented in O-band due to negligible CD impairment. However, it is universally acknowledged that C-band transmission has the advantages of lower fiber loss and more mature, commercially available lasers and dense wavelength division multiplexing (DWDM) optics [10,11]. Therefore, PON systems operating at C-band can potentially achieve lower cost and better receiver sensitivity than those at Oband, given that CD is well addressed by electrical equalization techniques. Meanwhile, both low complexity and effectiveness are crucial factors for equalization techniques considering that access network is extremely cost sensitive.

In this work, a  $50 \text{ Gb/s/}\lambda$  PAM4-PON with a low-cost 10 G class receiver is experimentally demonstrated in C-band. Memory polynomial equalizer (MPE) combined with decision feedback equalizer (DFE) is deployed at the receiver to mitigate channel distortions. A low-complexity hybrid decision scheme (HDS) including single-symbol decision (SSD) and multi-symbol decision (MSD) is first proposed to improve equalization performance. Experimental results show that the

<sup>&</sup>lt;sup>2</sup>School of Electrical and Computer Engineering, Georgia Institute of Technology, Atlanta, Georgia 30308, USA

<sup>\*</sup>Corresponding author: qiao@bupt.edu.cn

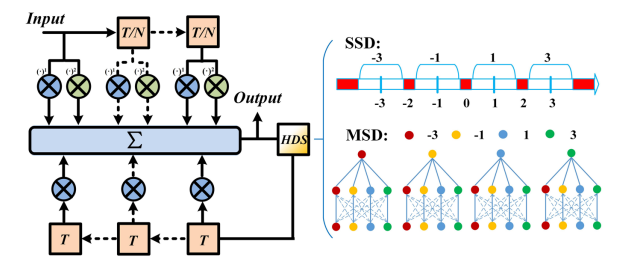


**Fig. 1.** Schematic structure of MPE-DFE with hybrid decision scheme.

HDS achieves a 0.7 dB and 1.3 dB sensitivity gain compared with SSD alone, and up to 35.4 dB and 31.4 dB link power budget, regarding the forward error correction (FEC) threshold of  $10^{-2}$  and  $10^{-3}$ , respectively.

Generally, the received signal after square-law detection in IM/DD systems can be expressed as [12]

$$r(t) = d_c^2 + |s(t) * h(t)|^2 + 2d_c s(t) * h(t) + n(t),$$
 (1)

where s(t) and r(t) are the transmitted and received signal, respectively,  $d_c$  is the direct current (DC) bias, h(t) is the channel response, and n(t) denotes system noise. In Eq. (1), the first term can be simply removed by a DC block, and the second term is a nonlinear distortion, namely a signal-to-signal beating interference. The most important information is contained in the third term. However, it suffers from channel distortions, which can be caused by insufficient system bandwidth, nonlinear response of electrical/optical devices, and fiber dispersion.

To mitigate the aforementioned distortions, an MPE-DFE with low-complexity HDS is proposed. Figure 1 shows the schematic structure of MPE-DFE, which includes the feedforward structure of MPE and the feedback structure of DFE. The mathematical form of MPE-DFE can be expressed as

$$y(n) = \sum_{k_1=0}^{K_1-1} h_{k_1} x(n-k) + \sum_{k_2=0}^{K_2-1} h_{k_2} x^2(n-k) + \sum_{l=1}^{L} f_l \hat{d}(n-l),$$

where x(n), y(n), and  $\hat{d}(n)$  are the input signal, output signal, and decision signal, respectively.  $K_1$  and  $K_2$  denote tap numbers;  $h_{k_1}$  and  $h_{k_2}$  represent tap coefficients for MPE; and L and  $f_l$  are the tap number and tap coefficients for DFE, respectively. In this equalizer, MPE based on a memory polynomial model is used to handle linear and nonlinear distortions while DFE is applied to mitigate enhanced system noise. However, a big issue for DFE is error propagation, which probably occurs when the feedback symbols are unreliable. We use  $\xi_r$  to represent the minimum distance between the output symbol y and the signal constellations  $S_c$ , which is calculated as

$$\xi_r = \min |\gamma - S_c|. \tag{3}$$

Furthermore, we define distance threshold  $D_T$  as a benchmark. In other words, the symbols are defined as unreliable symbols when  $\xi_r > D_T$ . Afterward, we propose to use SSD for reliable symbols and MSD for unreliable symbols, namely, HDS shown in Fig. 1. The SSD is exactly the conventional hard decision based on minimum Euclidean distance. As for MSD, we adopt total minimum mean square error (MSE) for several successive symbols instead of a single symbol. Since the

decision feedback depth is *L*, we choose *L* symbols together for MSD. The optimal decision symbols for MSD can be obtained through matrix calculation, which is expressed as

$$\begin{bmatrix} e(n) \\ e(n+1) \\ e(n+2) \\ \dots \\ e(n+L-1) \end{bmatrix} = \begin{bmatrix} y(n) \\ y(n+1) \\ y(n+2) \\ \dots \\ y(n+L-1) \end{bmatrix}$$

$$-\begin{bmatrix} 1 & 0 & \cdots & 0 \\ -f_1 & 1 & \cdots & 0 \\ -f_2 & -f_1 & \cdots & 0 \\ \vdots & \vdots & \ddots & \vdots \\ -f_{L-1} & -f_{L-2} & \cdots & 1 \end{bmatrix} \begin{bmatrix} \hat{d}(n) \\ \hat{d}(n+1) \\ \hat{d}(n+2) \\ \vdots \\ \hat{d}(n+L-1) \end{bmatrix}, \quad \textbf{(4)}$$

where e(n+i), y(n+i), and  $\hat{d}(n+i)$ ,  $i=0,\ldots,L-1$  represent the errors, the previous output symbols, and the candidate decision symbols, respectively. The optimal solution (i.e., the total minimum MSE,  $\sum_{i=0}^{L-1} e^2(n+i)$ ) can be achieved with a maximum likelihood detection (MLD) algorithm [13]. However, the complexity of full-MLD increases exponentially with the memory length, which restricts its practical application in cost-sensitive optical network units (ONUs). Besides, the final output of MSD can be either the first symbol or the whole L symbols. However, if the output of MSD is only one symbol, MSD becomes a sliding window, which results in a multiple increase in complexity. Hence, we adopt L symbols as output to reduce complexity.

Furthermore, a simplified MLD is proposed to reduce the complexity of MSD. Since the complexity of MLD is proportional to the required searching paths, the M-algorithm, which constrains the number of searching paths, can reduce the complexity. Given that each layer has S constellation candidates, the total searching paths for L layers would be  $S^L$ . The M-algorithm constrains the searching paths starting from the mth layer, which compares the MSE of following paths coming from the same upper-layer node, and only retains one path with the lowest MSE. In this way, the number of searching paths is limited to  $S^{m+1}$  ( $m+1 \le L$ ). The simplified MLD with M-algorithm is denoted as MLD-M(m). For instance, the inset of MSD in Fig. 1 shows a schematic diagram of MLD-M(2) with limited searching paths of  $S^3$ , in which the dashed lines denote the discarded paths, and the solid lines are the retained paths.

The number of multiplications is mainly evaluated to measure complexity for different decision schemes. For SSD, each output symbol needs  $K_1 + 2K_2 + L$  multiplications. As for MSD, first, these multiplications are still required to obtain previous output symbols. Then, extra multiplications are required to perform the MLD solution. Table 1 shows the comparison

Table 1. Number of Multiplications of Full-MLD and MLD-M(m) for *L* Output Symbols

Method	Calculating Errors for Possible Nodes	Square Operation of Errors
Full-MLD	$\frac{SL(L-1)}{2}$	$\frac{S(S^L-1)}{(S-1)}$
MLD-M(m)	$mS(L-m) + \sum_{k=0}^{m-1} kS$	$S^{m+1}(L-m) + \sum_{k=1}^{m} S^k$

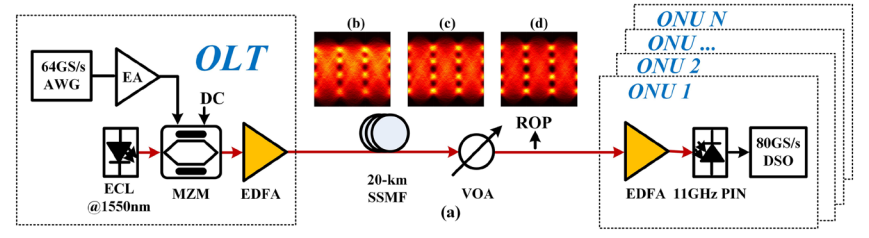


**Fig. 2.** (a) Experimental diagram of C-band 50 Gb/s PAM4-PON. (b)–(d) Inset eye diagrams @ -25 dBm with FFE, MPE, and MPE-DFE, respectively.

of multiplications between full-MLD and MLD-M(m) for L symbols. The multiplications come from two parts: one is the calculation of errors for possible decision symbols, and the other one is the square operation of these errors. Therefore, the number of multiplications of full-MLD would increase exponentially but MLD-M(m) would not. Moreover, the value of m can be optimized flexibly creating a tradeoff between complexity and accuracy.

Figure 2(a) shows the experimental setup of a C-band 50 Gb/s PAM4-PON system. At the optical line termination (OLT) side, 25 GBaud PAM4 symbols with Nyquist shaping are loaded into an arbitrary waveform generator (AWG) with a 64 GSa/s sampling rate and a 25 GHz bandwidth. After being amplified by a 40 GHz electrical amplifier (EA), a 25 GHz Mach-Zehnder Modulator (MZM) is used to modulate the electrical signal into the optical domain with an optical carrier at 1550 nm. An erbium-doped fiber amplifier (EDFA) is applied to boost the launch power to 8 dBm. Then, the optical signal is launched into a 20 km standard single-mode fiber (SSMF) for transmission. Afterward, a variable optical attenuator (VOA) is adopted to emulate the optical power splitting in the PON system. At the ONU side, a pre-amplified EDFA is used to extend the power budget, then followed by an 11 GHz PIN-photodiode and a digital storage oscilloscope (DSO) with an 80 GSa/s sampling rate and a 25 GHz bandwidth. Finally, the offline processing is processed in MATLAB. The inset Figs. 2(b)–2(d) shows recovered eye diagrams with oversampling at a received optical power (ROP) of -25 dBm with feed-forward equalizer (FFE), MPE, and MPE-DFE, respectively. The tap numbers have been optimized for each equalizer, namely, 41 taps for FFE, 41 taps of the first order and 21 taps of the second order for MPE, and five taps for DFE. Note that FFE/MPE operates at T/2 symbol intervals to provide robustness against clock jitter. Figure 2(b) shows that the eye diagram unevenly spreads out, because FFE can hardly equalize nonlinear distortions. However, the distribution of the eye diagram in Fig. 2(c) becomes more uniform thanks to nonlinear equalization of MPE. Moreover, the recovered eye diagram in Fig. 2(d) is clearer than that in Fig. 2(c), which indicates MPE-DFE mitigates enhanced noise due to the feedback structure.

To further improve performance for MPE-DFE, the conventional decision scheme of SSD is replaced by HDS, in which the output symbols are either determined by SSD or MSD depending on the distance threshold. Moreover, since MSD requires higher complexity than SSD, the MSD ratio in HDS is evaluated, which is defined as the number of symbols with MSD divided by the number of all output symbols. The variation of the distance threshold would change the MSD ratio. In other words,  $D_T = 0$  means 100% MSD, and  $D_T = 1$  depicts nearly 100% SSD. Figure 3 reveals the relationship of the bit error

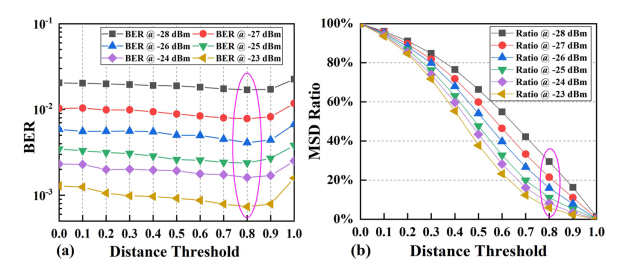


**Fig. 3.** BER and MSD ratio versus distance threshold for MPE-DFE.

ratio (BER) and MSD ratio versus distance threshold at different ROPs. Note that full-MLD is applied for MSD to achieve the best performance when sweeping the distance threshold. Figure 3(a) shows that the optimal performance is achieved when  $D_T=0.8$  at all of the ROPs. Hence, it would be convenient to implement HDS in a real application because there is a stable and optimal distance threshold to determine whether the output symbols are reliable. Figure 3(b) reveals the relationship between the MSD ratio and the distance threshold. The MSD ratio decreases as the distance threshold and the ROP increase. The MSD ratio would be less than 20% when the ROP is greater than -27 dBm at the optimized  $D_T$  of 0.8, which indicates MSD only accounts for a small percentage in HDS.

Although the MSD ratio is relatively low in HDS, the complexity of MSD with full-MLD increases exponentially with memory length. Therefore, a simplified MLD solution is investigated for MSD. Figure 4 shows BER versus ROPs from −28 dBm to −23 dBm with MPE-DFE using different decision schemes, in which the decision scheme of error propagation free (EPF) takes all the transmitter data for training, as a reference for other schemes. Among those decision schemes, SSD reaches the worst performance while HDS with different MSD schemes achieves a similar performance. In other words, MSD with MLD-M(1) achieves similar BER with both MLD-M(2) and full-MLD. However, MLD-M(1) only requires 84 multiplications, which reduces the complexity by ~94% compared with 1404 multiplications in full-MLD. Hence, the MSD with MLD-M(1) is applied in HDS considering the performance and complexity. Moreover, Fig. 4 reveals that the reference performance of EPF can be approached with HDS at higher ROPs, which indicates that HDS is more effective in cases of higher

Figure 5 shows the relationship between BER and ROP with different equalizers. In addition, the achieved receiver sensitivities and the required multiplications are presented in Table 2 to present a clear comparison. Considering a LDPC-FEC of  $10^{-2}$ , the FFE only achieves a sensitivity of -21.7 dBm after

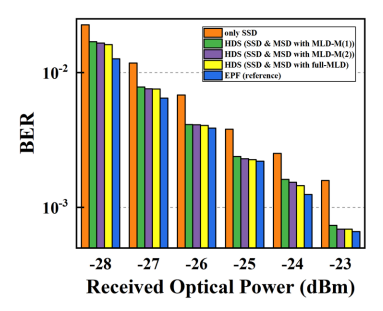


**Fig. 4.** BER versus received optical power with different decision schemes for MPE-DFE.

a 20 km fiber transmission. Thanks to the nonlinear equalization of MPE, the sensitivity significantly improves from  $\sim$ 4 dB to -25.7 dBm. Owing to the feedback structure of DFE, MPE-DFE achieves a 1 dB sensitivity gain compared with MPE. Moreover, MPE-DFE with HDS achieves a sensitivity of -27.4 dBm, which shows an additional 0.7 dB sensitivity gain compared with only SSD. In addition, if we consider a low-complexity RS(255,223) code with an FEC threshold of  $10^{-3}$ , both FFE and MPE cannot reach the limit when ROP is less than -21 dBm. Fortunately, MPE-DFE with conventional SSD reaches a sensitivity of -22.1 dBm whereas MPE-DFE with the proposed HDS achieves a sensitivity of -23.4 dBm. As a consequence, considering the launch power of 8 dBm, the proposed MPE-DFE with HDS achieves a power budget of  $35.4 \,\mathrm{dB}$  and  $31.4 \,\mathrm{dB}$  at FEC of  $10^{-2}$  and  $10^{-3}$ , respectively. The performance of optical back-to-back (BtB) transmission is also presented in Fig. 5, which is a reference to measure the power penalty for a 20 km transmission. It can be found that the power penalties with MPE-DFE using HDS are  $\sim$ 2 dB and  $\sim$ 2.5 dB at FEC of  $10^{-2}$  and  $10^{-3}$ , respectively. It is noted that SSMF loss at C-band is  $\sim 0.18 - 0.20$  dB/km while the loss at O-band is  $\sim$ 0.32 – 0.34 dB/km. As a result, a 20 km fiber transmission in C-band has an  $\sim$ 3 dB power margin than that operated in O-band. Hence, the proposed equalization scheme in C-band can potentially achieve a higher power budget than that in O-band. As for complexity, Table 2 shows that 88 and average 108.4 multiplications per output symbol are needed for SSD and MSD, respectively. This result indicates that MSD only increases 19.1% multiplications compared to SSD. Moreover, since MSD accounts for a small proportion in HDS, MPE-DFE with HDS only requires slightly higher complexity compared with the conventional SSD.

In conclusion, we have proposed a low-complexity HDS for MPE-DFE in a C-band  $50\text{Gb/s}/\lambda$  PON system with a low-cost

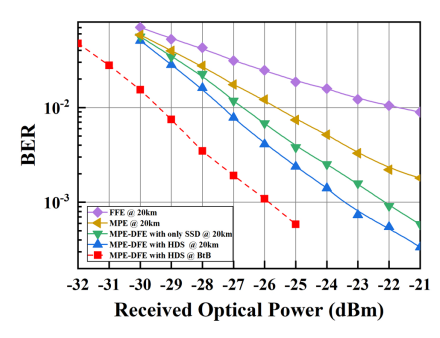


**Fig. 5.** BER versus received optical power with different equalizers.

Table 2. Comparison of Receiver Sensitivity and Multiplications Among Different Equalizations

Equalizations	Sensitivity @ 10 <sup>-2</sup>	Sensitivity @ 10 <sup>-3</sup>	Required Multiplications per Symbol
FFE	−21.7 dBm	N/A	41
MPE	$-25.7  \mathrm{dBm}$	N/A	83
MPE-DFE w/SSD	$-26.7  \mathrm{dBm}$	$-22.1  \mathrm{dBm}$	88
MPE-DFE w/HDS	−27.4 dBm	-23.4 dBm	88 for SSD 104.8 for MSD

10 Gb/s receiver. The HDS consists of two parts: SSD for reliable symbols and MSD for unreliable symbols. Experimental results show that there is an optimal distance threshold of 0.8 to determine whether the output symbol is reliable. We also find that the optimal MSD ratio is less than 20% when ROP is greater than -27 dBm. Moreover, to further reduce the complexity of MSD, the conventional full-MLD is replaced by a simplified MLD-M(1) algorithm, in which the number of multiplications reduces by  $\sim$ 94% compared to full-MLD with a similar performance. Finally, thanks to the effective equalization of MPE-DFE with HDS, we achieved power budgets of 35.4 dB and 31.4 dB at FEC limits of  $10^{-2}$  and  $10^{-3}$ , respectively.

**Funding.** National Natural Science Foundation of China (61771062, 61871044); Fund of State Key Laboratory of IPOC (BUPT) (No. IPOC2018ZT08); BUPT Excellent Ph.D. Students Foundation (CX2019311); China Scholarship Council.

**Disclosures.** The authors declare no conflicts of interest.

## **REFERENCES**

- 1. J. S. Wey, J. Lightwave Technol. 38, 31 (2020).
- E. Harstead, D. van Veen, V. Houstsma, and P. Dom, J. Lightwave Technol. 37, 657 (2019).
- D. van Veen and V. Houstsma, J. Opt. Commun. Netw. 12, A95 (2020).
- J. Zhang, K. Wang, Y. Wei, L. Zhao, W. Zhou, J. Xiao, B. Liu, X. Xin, and J. Yu, in *Optical Fiber Communication Conference (OFC)*, OSA Technical Digest (Optical Society of America, 2020), paper Th1B.3.
- B. Li, K. Zhang, D. Zhang, J. He, X. Dong, Q. Liu, and S. Li, J. Opt. Commun. Netw. 12, D1 (2020).
- E. Harstead, R. Bonk, S. Walklin, D. van Veen, V. Houtsma, N. Kaneda, A. Mahadevan, and R. Borkowski, J. Opt. Commun. Netw. 12, D17 (2020).
- J. Wei and E. Giacoumidis, in Optical Fiber Communication Conference (OFC), OSA Technical Digest (Optical Society of America, 2017), paper Tu3G.3.
- M. Tao, L. Zhou, H. Zeng, S. Li, and X. Liu, in Optical Fiber Communication Conference (OFC), OSA Technical Digest (Optical Society of America, 2017), paper Tu3G.2.
- J. Zhang, J. S. Wey, J. Yu, Z. Tu, B. Yang, W. Yang, Y. Guo, X. Huang, and Z. Ma, in *Optical Fiber Communication Conference (OFC)*, OSA Technical Digest (Optical Society of America, 2018), paper M1B.4.
- X. Tang, Y. Qiao, J. Zhou, M. Guo, J. Qi, S. Liu, X. Xu, and Y. Lu, Opt. Express 26, 33418 (2018).
- J. Zhang, J. Yu, J. Shi, J. S. Wey, X. Huang, Y. Guo, Z. Ma, and M. Li, in European Conference on Optical Communication (ECOC) (2017), p. 1.
- R. Rath, D. Clausen, S. Ohlendorf, S. Pachnicke, and W. Rosenkranz, J. Lightwave Technol. 35, 3909 (2017).
- X. Tang, Y. Qiao, Y. Chen, Y. Lu, and G. Chang, J. Lightwave Technol. 38, 4683 (2020).